ISSN 1070-3632, Russian Journal of General Chemistry, 2014, Vol. 84, No. 10, pp. 2031–2036. © Pleiades Publishing, Ltd., 2014.

Study on Synthesis of Superparamagnetic Spinel Cobalt Ferrite Nanoparticles as Layered Double Hydroxides by Co-precipitation Method[1]

H. A. Hamad[a], M. M. Abd El-latif[a], A. B. Kashyout[b], W. A. Sadik[c], and M. Y. Feteha[c]

[a] *Fabrication Technology Department, Advanced Technology and New Materials Research Institute, City of Scientific Research and Technological Applications (SRTA-City), New Borg El-Arab City, P.O. Box 21934, Alexandria, Egypt*
e-mail: heshamaterials@hotmail.com

[b] *Electronic Materials Department, Advanced Technology and New Materials Research Institute, City of Scientific Research and Technological Applications (SRTA-City), New Borg El-Arab City, P.O. Box 21934, Alexandria, Egypt*

[c] *Materials Science Department, Institute of Graduate Studies and Research (IGSR), Alexandria University, 163 Horrya Avenue, P.O. Box 832, Shatby, 21526 Alexandria, Egypt*

Received April 16, 2014

Abstract—Cobalt ferrite layered double hydroxide (LDH) nanoparticles with cubic structure were synthesized by the co-precipitation method: addition of NaOH solution to a solution of Co^{2+} and Fe^{3+}. Formation of nanoparticles was confirmed by XRD, SEM, TEM, PSA, FT-IR, TGA, DSC, and magnetic characteristics were measured using VSM. Crystals produced by calcination at 900°C possessed high coercivity and pronounced physical and chemical stability. Nanoparticles of $CoFe_2O_4$ formed outer layers with poor crystallization on the surface of cobalt ferrite nanocrystals.

Keywords: magnetic materials, chemical synthesis, X-ray diffraction, magnetic properties

DOI: 10.1134/S1070363214100296

INTRODUCTION

Layered double hydroxides (LDHs) are solid base catalysts of high potential that have the general formula $[M^{II}_{1-x}M_x^{III}(OH)_2]^{z+}A^{n-}_{z/n}\cdot yH_2O$, where M^{II} and M^{III} are metal cations, x is defined as $M^{II}/(M^{II} + M^{III})$ ratio generally varies from 1 to 5. The layer charge is $z = x$ when the M^{II} is a divalent cation and $z = 2x - 1$ when A^{n-} denotes anions. LDHs consist of brucite-like layers in which M^{II} cations are partially substituted by M^{III} cations resulting in a net positive charge which is compensated by interlayer anions of the hydrated interlayer region. The basic properties of LDHs and materials derived from those can be tailored by altering nature of the cations in the layers, M^{II}/M^{III} ratio, nature of anions, and activation conditions [1].

Recently application of spinel ferrites has been intensively studied in such areas as high-density information storage system [2], ferrofluid technology [3], magnetocaloric refrigeration [4], medical diagnostics [5], magnetic resonance imaging enhancement [6], and gas sensors [7]. Generally, magnetic properties of ferrite are highly dependent on particles microstructure and volume, surface to volume ratio, intra- and intergranular pores [8].

Among spinel ferrites cobalt ferrite $CoFe_2O_4$ is of considerable interest due to its large magnetocrystalline anisotropy (2.65×10^6–5.1×10^6 erg/cm^3) [9], high coercivity at 4.3 kOe at room temperature [10], moderate saturation magnetization (M_s = 80 emu/g) [11], large magnetostrictive coefficient [12], chemical stability, and mechanical hardness. It exhibits higher coercivity than the other spinel ferrites [13–15]. $CoFe_2O_4H$ as an inverse spinel structure in which oxygen atoms make up an FCC lattice with half of Fe^{3+} ions occupying the tetrahedral A sites and the other half together with Co^{2+} ions located at the octahedral B sites.

LDHs can be easily synthesized by co-precipitation of a solution of bivalent and trivalent metal salts with a

[1] The text was submitted by the authors in English.

base (NaOH or KOH) [16]. Generally, supersaturation conditions are reached by controlling pH of the solution [17]. High catalytic activity of particles is related directly with their surface and structural properties such as small size, high surface area, shape and size distributions of pores [18]. Various synthesis strategies for magnetic nanoparticles had been studied [19–26]. Co-precipitation is the simplest method for spinel iron nanoparticles with size range 5–180 nm [27]. This can be the most promising method due to its simplicity, efficiency, and simple control of size and shape of particles. The latter depends on the type of iron salts used (chlorides, sulfates, nitrates, perchlorates, etc.), Fe^{2+}/Fe^{3+} ratio [28], presence of oxygen gas, reaction rate and temperature [18].

In this study $CoFe_2O_4$ particles have been synthesized by chemical co-precipitation method under different temperatures. XRD has been used to evaluate crystalline structure and purity of the prepared phases. Magnetic characters of the samples have been evaluated.

EXPERIMENTAL

Materials and methods. Suppliers of the chemicals: $[Co(NO_3)_2 \cdot 6H_2O]$, 98%, Belami Fine Chemicals (India); $[FeCl_2 \cdot 4H_2O]$, 99%, ACROS Chemicals (USA-Belgium); $[FeCl_3 \cdot H_2O]$, min. 99%, Riedel-Dehaen–Sigma Aldrich Chemicals (Switzerland).

Cobalt spinel ferrite nanoparticles were synthesized as follows: $Co(NO_3)_2 \cdot 6H_2O$, $FeCl_2 \cdot 4H_2O$, and $FeCl_3 \cdot H_2O$ with molar ratio of cations $Co^{2+} : Fe^{2+} : Fe^{3+}$ = 1.9 : 1 : 2 were dissolved together in de-ionized water (18.2 MΩ cm). Aqueous solution of NaOH (1.5 mol/L) was added drop wise under N_2 to pH 7.0 to ensure complete precipitation. The slurry formed was removed from a three neck flask and stored at 40°C for 4 h to improve crystallinity. The precipitate was filtered off, washed with deionized water and ethanol and dried at 50°C under vacuum for 24 h. The resulting LDHs precursor was calcinated at 900°C for 2 h to give $CoFe_2O_4$ LDHs nanoparticles.

Instruments. pH Was measured by a single electrode pH-meter (Denver Instrument Co., USA). X-ray diffraction analysis was carried out with Shimadzu-XRD-7000 Diffractometer (Japan), at room temperature with CuK_α radiations of wavelength (λ = 1.5406 Å), generated at 30 kV–30 mA for cobalt ferrite nanoparticles. The nanoparticle size distribution was measured by Beckman Coulter N5 submicron particle size analyzer, USA. Morphology of the synthesized powders was studied by SEM scanning electron microscope (JEOL JSM-6360 LA, Japan) with a power supply of 30 kV. The composition and elemental studies of $CoFe_2O_4$ nanoparticles were carried out by EDAX combined with the scanning electron microscopy and TEM transmission electron micro-scope (JEOL JEM 1230, Japan) with Max. Mag. 600k× and resolution 0.2 nm. FT-IR spectra were recorded by FTIR spectrophotometer Shimadzu-8400 S (Japan) in KBr tablets. Thermal characteristics were measured by TGA-50H, Shimadzu (Japan) with heating rate 10°C/min (30 mL/min) up to 600°C under N_2. DSC was performed with a heat flux Shimadzu DSC-60A, (Japan) in N_2 atmosphere, flow rate 30 mL/min, temperature range 30–600°C and heating rate 10°C/min. Magnetic characteristics were measured by VSM (Lake Shore-7410 vibrating sample magnetometer), magnetic field up to 20 kOe and magnetic moment sensitivity up to 1 memu.

RESULTS AND DISCUSSION

Effect of pH on synthesis of $CoFe_2O_4$·LDHs nanoparticles. pH Of the initial reactant solution was 2.2, upon slow addition of NaOH it increased slowly to 2.7 and then rapidly to 6.6**.** Evidently, pure $CoFe_2O_4$ was synthesized at pH 7**.** The method of NaOH addition had a significant influence on the nucleation rate. High concentration of OH^- could lead to lower nuclei concentration of $Fe^{3+}$and Co^{2+}.

On the basis of pH titration curves of the mixed salt solutions by NaOH the hydroxide ion reacted with aqueous M^{II} ions at higher pH to give the LDH. Generally the LDHs are thermodynamically unfavorable for mixtures of metal hydroxides, but mass action effects associated with the high concentration of an anion drive the system towards the LDH [17].

Effect of calcinations temperature on preparation of $CoFe_2O_4$ nanoparticles. ***Structure and properties of magnetic core $CoFe_2O_4$ nanoparticles.*** *XRD*. According to powder X-ray diffraction (XRD) all three precursors had the characteristic structure of hydrotalcite-like compounds. The synthesized $CoFe_2O_4$ had the structure similar to that of MgFe–LDH with Mg : Fe ratio 1 : 2. It exhibited crystallinity poorer than that with Mg : Fe ratio 2 : 1 or 1 : 1 due to higher charge density in the layers [18]. Spinel phase diffraction peaks were registered within shorter time upon higher concentration of MFe_2O_4. The mean

crystals size was calculated from the diffraction peak width by the Scherrer's equation [29].

$$L = k\lambda/(\beta\cos\theta), \quad (1)$$

where (L) is a crystals size, (λ) is a wavelength of the X-ray radiation, (β) is the line width at half-height, (θ) is a diffraction angle, k = 0.89, shape factor for spherical particles. $CoFe_2O_4$ Structure is typical to that of the inverse spinel group with the general formula A $(B_2)O_4$. The peaks at 18.2°, 30.0°, 35.4°, 37.2°, 43.47°, 57.1°, and 62.72° were attributed to (111), (220), (311), (222), (400), (511), and (440) reflections of the spinel phase of $CoFe_2O_4$.

The peaks stood for the cubic structure (space group: Fd-*3m*) typical for $CoFe_2O_4$ crystals (JCPDS no. 003-0864). In accordance with the Sherrer's formula size of spinel crystals was about 10–12 nm (Table 1), space group Fd3. Its amorphous character vanished and the diffraction peak of (311) crystal plane showed up. The diffraction peak matched the JCPDS standard card, but it was relatively broad which indicated that $CoFe_2O_4$ crystallization remained incomplete with crystal defects and smaller crystals size ca 23.1 nm. At 900°C the peak was relatively narrow and high, which indicated that the crystals growth progressed and completed. The crystalline phase was stable [30]. The average crystals size grew accordingly [31, 32].

Particles size. Calcination at 800°C resulted in formation of ca 44 nm particles that grew up to 1.1 mm at 1000°C (Fig. 1). At the higher end of that range the resulting cobalt ferrite particles growth rate exceeded the nucleation rate (Table 2). The size of particles increased linearly with calcination temperature growth.

Morphology of $CoFe_2O_4$. SEM images of $CoFe_2O_4$ have uniform spherical structure morphology (Fig. 2) with spherical particles of narrow size distribution (52–90 nm) at 900°C. The element analysis detected the following elements: Co (11.31%), Fe (25.52%) and O (63.18%) corresponding to $CoFe_2O_4$.

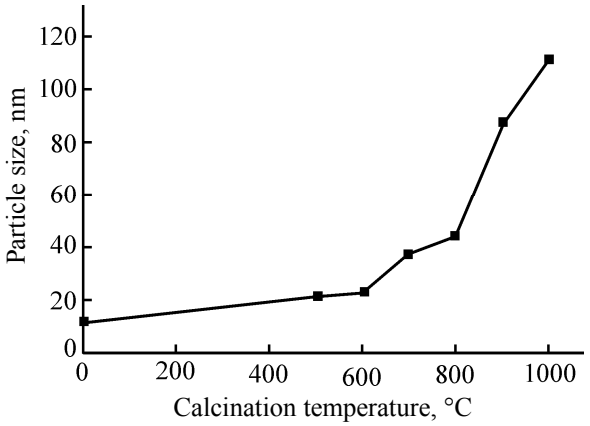

Fig. 1. Particle size (nm) as function of calcination temperatures (°C) of $CoFe_2O_4$ LDHs nanoparticles.

TGA and DSC. The TGA curve demonstrated three stages of weight loss. The first stage at 25–120°C was associated with dehydration of the sample (weight loss 7.8%), the second one between 120 and 270°C, was attribute to decomposition of nitrates (7.2% weight loss) and start of cobalt ferrite crystallization and the third stage between 269 and 600°C corresponded to the loss of structural water. Above 600°C no weight loss was observed and crystallization process was completed**.**

In DSC the exothermic peak with maximum at 113.23°C was attributed to hydration and loss of water with specific 30.13 j/g.

IR spectra. A band centered around 1383 cm^{-1} indicated the presence of NO_3^- ions [33] and C–H bond in the gel [34]. The metal-oxide vibration band characteristic to cobalt ferrite (580 and 370 cm^{-1}) was attributed to the spinel structure.

Table 1. XRD and yield results of as prepared and calcined $CoFe_2O_4$

Sample	Calcination temperature, °C (1 h)	Crystalline size[a], nm	Particle size[b], nm	Yield after calcinations, %
1C	0	–	11.5	–
1C2	600	19.59	23.1	73.55
1C5	900	37.57	87.4	69.33

[a] Calculated by the Scherrer equation. [b] Determined by particle size analyzer.

Table 2. Magnetic properties of as prepared $CoFe_2O_4$ and calcined at 900°C

Sample	Corecivity, kOe	Remnant magnetization M_r, emu/g	Saturation magnetization M_s, emu/g
1C	0.02	0.30	13.60
1C5	1.25	29.49	70.63

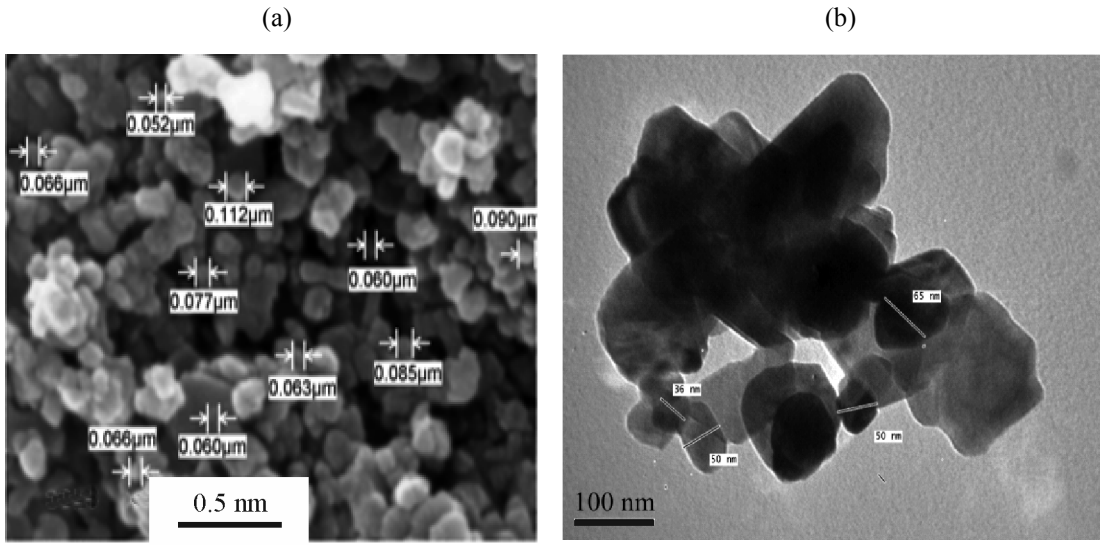

Fig. 2. (a) SEM and (b) TEM micrograph as calcined $CoFe_2O_4$ LDHs nanoparticles at 900°C.

VSM. Magnetic properties of as-prepared $CoFe_2O_4$ nanoparticles and those calcinated at 900°C were studied with a quantum magnetometer VSM at 300 K ($T > T_B$) with maximum applied field up to 20 kOe are presented in Fig. 3. The coercivity (H_c) was about 0.0237and1.2506 kOe. Saturation magnetization (M_s) values were ca 13.6 and 70.628 emu/g and indicative of strong soft magnetic properties [18] with the remnant magnetization (M_r), 0.3and 29.49 emu/g. The magnetic structure of crystals was unstable and in disorder. The magnetic moment could not be maintained consistent with the external field. The crystal structure did not change under the action of magnetic field and pressure applied [36].

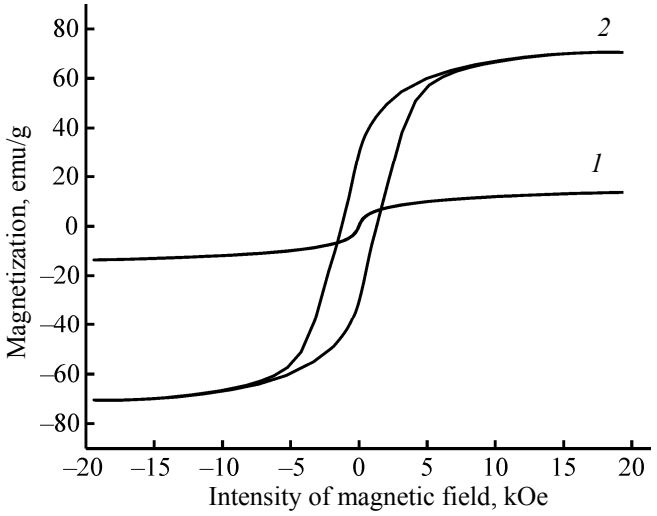

Fig. 3. Magnetization vs. Magnetic Field of (*1*) as prepared $CoFe_2O_4$ LDHs nanoparticle, and (*2*) as calcined at 900°C.

According to reversibility of the M–H curve recorded at room temperature the sample was superparamagnetic. $CoFe_2O_4$ Crystals of less than 14 nm size demonstrated superparamagnetic character at room temperature.

The remanence ratio 0.41 for calcinated cobalt ferrite was close to the expected one (0.5) for a system of non-interacting single domain particles with uniaxial anisotropy though cobalt ferrite itself had the cubic structure [32]. Effectively uniaxial anisotropy in magnetic nanoparticles was attributed to surface effects as evidenced by simulations of nanoparticles [37].

Reaction mechanism. The reaction of $Co(NO_3)_2 \cdot 6H_2O$, $FeCl_2 \cdot 4H_2O$, and $FeCl_3 \cdot 6H_2O$ with NaOH solution at pH 7 may follow three possible pathways [38].

(a) Dissolution of $Co(NO_3)_2 \cdot 6H_2O$, $FeCl_2 \cdot 4H_2O$, and $FeCl_3 \cdot 6H_2O$ in water (liquid phase synthesis).

$$Co(NO_3)_2 \cdot 6H_2O \rightarrow Co(H_2O)_6^{2+} + 2NO_3^-, \quad (2)$$

$$FeCl_2 \cdot 4H_2O + 2FeCl_3 \cdot 6H_2O \rightarrow 3Fe(H_2O)_6^{3+} + 8Cl^- + 4H_2O. \quad (3)$$

The first path is a homogeneous phase reaction of $Co(NO_3)_2 \cdot 6H_2O$, $FeCl_2 \cdot 4H_2O$, and $FeCl_3 \cdot 6H_2O$ {Eqs. (2), (3), (8)–(10) [39]} that leads to homogeneous precipitation. Upon saturation the process

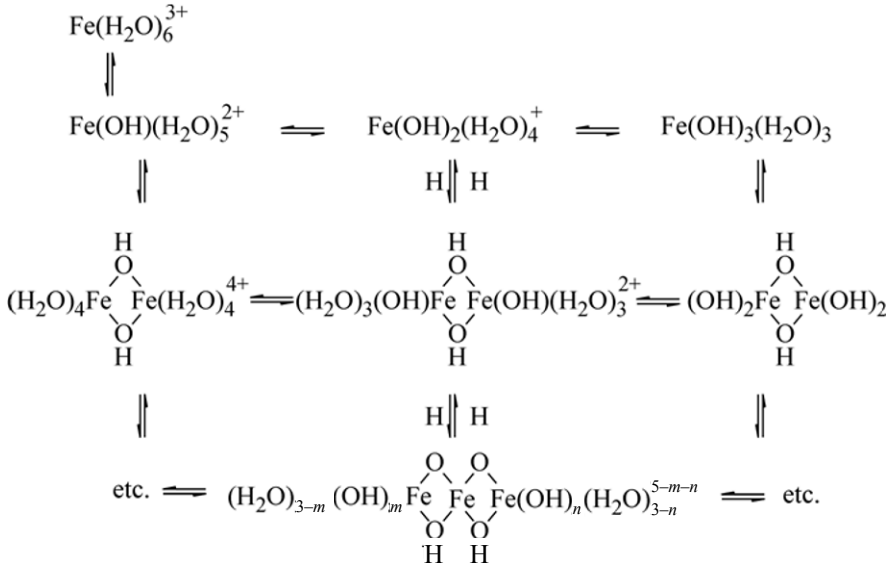

Fig. 4. Schematic digramm of the hydrolysis of iron.

reaches a point of nucleation. Particles growth progresses due to diffusion of atoms onto the nuclei and irreversible aggregation of nuclei.

This overall reaction proceeds in two steps: hydrolysis of the metal cations and subsequent dehydration to form oxides [40].

$$M^{n+} + nOH^- \rightarrow M(OH)_n, \quad (4)$$

$$M(OH)_n \rightarrow MO_{n/2} + (n/2)H_2O. \quad (5)$$

Dehydration. The second step involves formation of oxygen bridges between the metal cations. Mechanism of this step is unclear. However, it is assumed to be a reaction between two hydroxide ligands [40].

$$\sim Fe–OH + HO – Fe \rightarrow \sim Fe–O–Fe\sim + H_2O \quad (6)$$

or a deprotonation reaction

$$\sim Fe–OH–Fe\sim \rightarrow \sim Fe–O–Fe\sim + H^+. \quad (7)$$

(b) Transformations of the reactant solution combined with NaOH solution:

$$Co(H_2O)_6^{2+} + NaOH \rightarrow Co(OH)_x^{2-x} + NaOH \rightarrow Co(OH)_2\downarrow + NaOH \rightarrow Co(OH)^{3-}, \quad (8)$$

$$Fe(H_2O)_6^{3+} + NaOH \rightarrow Fe(OH)_y^{3-y} + NaOH \rightarrow Fe(OH)_2\downarrow + NaOH \rightarrow Fe(OH)^{3-}. \quad (9)$$

The second path is a solid–liquid two-phase phase reaction. $CoFe_2O_4$ is formed in the reaction of Co_3O_4, $FeCl_2 \cdot 4H_2O$ with $FeCl_3 \cdot 6H_2O$ in supercritical water [Eqs. (2)–(5), (11), and (12)].

(c) Reaction (*i*):

$$Co(OH)^{3-} + 2Fe(OH)^{4-} \rightarrow CoFe_2O_4\downarrow + 4H_2O + 3OH^-. \quad (10)$$

(d) Reaction (*ii*):

$$6Co(OH)^{3-} + O_2 \rightarrow 2Co_3O_4\downarrow + 6OH^- + 6H_2O, \quad (11)$$

$$2Co_3O_4 + 12Fe(OH)^{4-} \rightarrow 6CoFe_2O_4\downarrow + 12OH^- + 18H_2O + O_2\uparrow. \quad (12)$$

(e) Reaction (*iii*):

$$2Fe(OH)^{3-} \rightarrow Fe_2O_3\downarrow + 3H_2O, \quad (13)$$

$$Fe_2O_3 + Co(OH)^{3-} \rightarrow CoFe_2O_4\downarrow + OH^- + H_2O. \quad (14)$$

The third path is synthesis of $CoFe_2O_4$ from $Co(NO_3)_2 \cdot 6H_2O$ [Eqs. (2)–(5), (13), and (14)].

$$FeCl_2 + 2FeCl_3 + 3/2Co(NO_3)_2 + 8NaOH \rightarrow 3/2CoFe_2O_4 + 3NaNO_3 + 8NaCl + H_2O. \quad (15)$$

CONCLUSIONS

In summary, $CoFe_2O_4$ LDHs nanoparticles with spinel structure were synthesized by the co-precipitation method at pH = 7 and calcinated at 900°C and exhibited high superparamagnetic properties, physical and chemical stability. The crystallization, saturation magnetization, coercivity and remnant magnetization increased along with calcination temperature.

ACKNOWLEDGMENTS

This study has been done under the project funded by the Science and Technology Development Fund (STDF), Ministry of Scientific Research, Project ID: 1414, “Quantum Dots Nanomaterials Dye Sensitized Solar Cells.”

REFERENCES

1. Zhang, H., Qi, R., Evans, D.G., and Duan, X., *J. Solid State Chem*., 2003, vol. 177, p. 772.
2. Zolio, R.F., US Patent no. 474, 1984, p. 866.
3. Raj, K., Moskowitz, B., and Casciari, R., *J. Magn. Magn. Mater*., 1995, vol. 149, p. 174.
4. Mamiya, H., Terada, N., Furubayashi, T., Suzuki, H.S., and Kitazawa, H., *J. Magn. Magn. Mater*., 2010, vol. 322, nos. 9–12, p. 1561.
5. Bulte, J.W.M., *J. Magn. Reson. Imaging*, 1994, vol. 4, p. 497.
6. Kim, D., Zeng, H.,Ng, T.C., and Brazel, C.S., *J. Magn. Magn. Mater*., 2009, vol. 321, no. 23, p. 3899.
7. Patil, J.Y., Nadargi, D.Y., Gurav, J.L., Mulla, I.S., and Suryavanshi, S.S., *Mater. Lett*., 2014, vol. 124, no. 1, p. 144.
8. Xiao, S., H., Xu, H., J., Huc, J., Li , L., Y., and Li, X., *J. Physica E*, 2008, vol. 40, p. 3064.
9. Melikhov, Y., Snyder, J.E., Jiles, D.C., Ring, A.P., Paulsen, J.A., Lo, C.C.H., and Dennis, K.W., *J. Appl. Phys*., 2006, vol. 99, p. 08R102.
10. Chinnasamy, C.N., Jeyadevan, B., Perales-Perez, O., Shinoda, K., Tohji, K., and Kasuya, A., *IEEE Trans. Magn*., 2002, vol. 38, p. 2640.
11. Cullity, B.D., *Introduction to Magnetic Materials*, New York: Addision–Wesley, 1972.
12. Mohaideen, K.K. and Joy, P.A., *Curr. Appl. Phys*., 2013, vol. 13, no. 8, p. 1697.
13. Cao, X., J. Meng, J., Mi, F., Zhang, Z., and Sun, J., *Solid State Commun*., 2011, vol. 151, no. 9, p. 678.
14. Imine, S., Schoenstein, F., Mercone, S., Zaghrioui, M., Bettahar, N., and Jouini, N., *J. Eur. Ceram. Soc*., 2011, vol. 31, no. 15, p. 2943 .
15. Ayyappan, S., Philip, J., and Raj, B., *Mater. Chemi. and Phys*., 2009, vol. 115, p. 712.
16. Xu, Y., Zhang, H., Duan, X., and Ding, Y., *Mater. Chem. Phys*., 2009, vol. 114, nos. 2–3, p. 795.
17. Jing, H., Min, W., Li, B., Kang, Y., David, G.E., and Xue, D., *Struct. Bond*, 2006, vol. 119, p. 89.
18. Hui, Z., Rong, Q., David, G.E., and Xue, D., *J. Soli. State Chem*., 2004, vol. 177, p. 772.
19. Philip, J., Jaykumar, T., Sundaram, P.K., and Raj, B., *Meas. Sci. Technol*., 2003, vol. 14, p. 1289.
20. Sharifi, I., Shokrollahi, H., Doroodmand, M.M., and Safi, R., *J. Magn. Magn. Mater*., 2012, vol. 324, no. 10, p. 1854.
21. Ahmed, S.R. and Kofinas, P., *Mater. Res. Soc. Symp. Proc*., 2001, 661, KK 10.10.1.
22. Everett, E.C., *PhD Thesis (Chemistry)*, New Orleans Univ., Louisiana, USA, 1994.
23. Ibrahim, A.M., Abd El-Latif, M.M., and Mahmoud, M.M., *J. Alloys. and Comp*., 2010, vol. 506, p. 201.
24. Philip, J., Shima, P.D., and Raj, B., *J. Appl. Phys*., 2007, vol. 91, p. 203108.
25. Pitaa, M., Abad, J.M., Vaz-Dominguez, C., Briones, C., Mateo-Martí, E., Martín-Gago, J.A., del, M., Morales, P., and Fernandez, V.M., *J. Colloid Interface Sci*., 2008, vol. 321, p. 484.
26. Beck, H.P., Eiser, W., and Haberkorn, R., *J. European Ceramic Soc*., 2001, vol. 21, p. 687.
27. Gupta, A.K. and Gupta, M., *Biomaterials*, 2005, vol. 26, p. 3995.
28. Liu, Z.L., Wang, H.B., and Lu, Q.H., *J. Magn Magn Mater*., 2004, vol. 283, p. 258.
29. Buzby, S.E., *PhD Thesis (Materials Science and Engineering)*, Univ. of Delaware, Delaware, USA, 2005.
30. Zhao, L.J. and Jiang, Q., *J. Magn Magn Mater*., 2010, vol. 322, p. 2485.
31. Sort, J., Surmach, S., Munoz, J.S., and Baro, M.D., *Phys. Rev. B*, 2002, vol. 65, p. 174420.
32. Maaz, K., Arif, M., Hasanaina, S.K., and Ceylan, A., *J. Magn. Magn. Mater*., 2007, vol. 308, p. 289.
33. Xiao, S.H., Xu, H.J., Hu, J., Long, Y.L., and Xin, J.L., *Physica E*, 2008, vol. 40, p. 3064.
34. Hoffmann, M.R., Martin, S.T., Choi, W., and Bahnemann, D.W., *Chem. Rev*., 1995, vol. 95, p. 96.
35. Cot, F., Larbot, A., Nabias, G., and Cot, L., *J. Eur. Ceram. Soc*., 1998, vol. 18, p. 2175.
36. Cornell, R.M. and Schwertmann, U., T*he Iron Oxides: Structure, Properties, Reactions, Occurrences and Uses*, New York: VCH Publishers, 1996.
37. Kodama, R.H., Berkowitz, A.E., McNiff, E.J., and Foner, S., *Phys. Rev. Lett*., 1996, vol. 77, p. 394.
38. Beydoun, D. and Amal, R., *J. Mol. Catal. A: Chem*., 2002, vol. 180, p. 193.
39. Spanhel, L., Haase, M., Weller, H., and Henglein, A., *J. Am. Chem. Soc*., 1987, vol. 109, p. 5649.
40. Blesa, M.A. and Matijevic, E., *Adv. Colloid. Interface Sci*., 1989, vol. 29, p. 173.